Received: 16 July 2016 | Revised: 26 May 2017 | Accepted: 25 July 2017

DOI: 10.1002/oca.2355

RESEARCH ARTICLE

WILEY

Optimal control of heart rate during treadmill exercise

Kenneth J. Hunt | Ming Liu

Institute for Rehabilitation and Performance Technology, Division of Mechanical Engineering, Department of Engineering and Information Technology, Bern University of Applied Sciences, CH-3400 Burgdorf, Switzerland

Correspondence
Kenneth J. Hunt, Institute for Rehabilitation and Performance Technology, Division of Mechanical Engineering, Department of Engineering and Information Technology, Bern University of Applied Sciences, CH-3400 Burgdorf, Switzerland.
Email: kenneth.hunt@bfh.ch

Summary

Feedback control of heart rate (HR) for treadmills is important for exercise intensity specification and prescription. This work aimed to formulate HR control within a stochastic optimal control framework and to experimentally evaluate controller performance. A quadratic cost function is developed and linked to quantitative performance outcome measures, namely, root-mean-square tracking error and average control signal power. An optimal polynomial systems design is combined with frequency-domain analysis of feedback loop properties, with focus on the input sensitivity function, which governs the response to broad-spectrum HR variability disturbances. These, in turn, are modelled using stochastic process theory. A simple and approximate model of HR dynamics was used for the linear time-invariant controller design. Twelve healthy male subjects were recruited for comparative experimental evaluation of 3 controllers, giving 36 tests in total. The mean root-mean-square tracking error for the optimal controllers was around 2.2 beats per minute. Significant differences were observed in average control signal power for 2 different settings of the control weighting (mean power 22.6 vs 62.5×10^{-4} m^2/s^2, high vs low setting, $p = 2.3 \times 10^{-5}$). The stochastic optimal control framework provides a suitable method for attainment of high-precision, stable, and robust control of HR during treadmill exercise. The control weighting can be used to set the balance between regulation accuracy and control signal intensity, and it has a clear and systematic influence on the shape of the input sensitivity function. Future work should extend the problem formulation to encompass low-pass compensator and input sensitivity characteristics.

KEYWORDS

heart-rate control, optimal control, physiological control, polynomial approach, sensitivity functions, treadmills

1 | INTRODUCTION

Heart rate (HR) is a convenient variable to use for exercise intensity specification and prescription both in healthy individuals[1,2] and in patient populations.[3] High-intensity interval training protocols, for example,[4,5] combine various

*Notation and Abbreviations: q^{-1}, backward shift operator (time domain); $\nabla(q^{-1}) = 1 - q^{-1}$, backward difference operator; $\nabla[x](t) = (1 - q^{-1})x(t) = x(t) - x(t-1)$; z, z-transform complex variable (frequency domain); s, Laplace transform complex variable (frequency domain); $X^*(q^{-1}) = X(q), X^*(z^{-1}) = X(z)$, conjugate polynomial (discrete); P_d, nominal plant transfer function; C, feedback compensator transfer function; C_{pf}, deterministic reference prefilter transfer function; y, controlled variable (heart rate, HR); y_{nom}, HR_{nom}, nominal (simulated) heart-rate response; u, control signal (treadmill speed command, v); d, plant output disturbance; ψ_d, stochastic process, disturbance generator; r, reference signal (target heart rate, HR^*); r', filtered reference signal; e', feedback compensator input signal; u', sample-to-sample change in control signal; $u'(t) = \nabla[u](t) = u(t) - u(t-1)$; RMSE, root-mean-square tracking error; $P_{\nabla u}$, average power of changes in the control signal u, "average control signal power"; ANOVA, analysis of variance; bpm, beats per minute; HR, heart rate; HRV, heart-rate variability; LQ, linear quadratic; LTI, linear time invariant; PA, pole assignment.

HR intensity regimes of differing durations. Treadmills provide a useful platform for a systematic and automated implementation of such protocols, especially when combined with continuous feedback control of HR.

A variety of design methods have previously been investigated for feedback control of HR during treadmill exercise; implementations typically involve real-time monitoring of HR and continuous adjustment of a control variable, which is usually the treadmill speed command. The feedback designs that have been applied include classical proportional-integral (PI) control,[6] robust control in combination with a nonlinear state-space model,[7] model predictive control with a Hammerstein model structure,[8] and other forms of nonlinear control.[9] The design focus in these approaches has been on possible structural and parametric sources of uncertainty, ie, on whether the plant should be considered to comprise higher order and/or nonlinear components and whether the parameters within a given structure are subject to substantial variation.

In contrast, the primacy of broad-spectrum physiological HR variability (HRV) as a disturbance source and, therefore, its role as the principal feedback design challenge have been asserted elsewhere[10]: the observations therein were supported by empirical results, which used quantitative performance outcome measures, control designs based on simple and approximate linear time-invariant (LTI) plant models,[11] and subject cohorts of sufficient size to facilitate comparative statistical analysis. Furthermore, a direct head-to-head comparative study of linear and nonlinear controllers did not reveal any significant differences in performance outcomes at moderate exercise intensity.[12] These results have demonstrated that accurate, stable, and robust HR control performance can be obtained using simple models and LTI design methods, provided that the HRV disturbance spectrum is appropriately dealt with.

In the present work, the HR control problem is formulated within a stochastic optimal control framework using polynomial systems theory[13]; this is a linear quadratic (LQ) optimal approach based on a linear plant model and a quadratic cost function. This control design strategy, which is based on a cost function that can be expressed in both the time and frequency domains, is combined with frequency-domain analysis of feedback loop properties; particular attention is given to the shape of the input sensitivity function, which governs the behaviour of the control signal in response to broad-spectrum disturbances generated by physiological HRV. Heart-rate variability disturbances, in turn, are modelled conveniently using concepts from stochastic process theory.

Quantitative time-domain outcomes are again used for objective assessment of empirically observed controller performance: these comprise root-mean-square tracking error (RMSE) and average control signal power. An explicit link is drawn between these performance outcome measures and the quadratic objective function used in the optimal controller design: RMSE and average control signal power are shown to provide sample estimates of the quadratic terms within the cost function, with their relative importance being set through the choice of the control weighting design parameter.

Taking these 2 factors together, ie, the suitability of stochastic processes for modelling HRV disturbances and the link between appropriate outcome measures and the cost function, the stochastic optimal control framework is seen to provide a natural means by which to formulate the key elements of the HR control problem.

The aims of this work were to formulate HR control within the stochastic optimal control framework and, in an experimental evaluation study, to statistically compare quantitative performance outcomes obtained with 2 parameterisations of the optimal controller and with a direct pole-assignment (PA) controller.

2 | CONTROL DESIGN METHODS

2.1 | Nominal plant model

The optimal control problem formulation comprises the definition of a nominal plant model, a controller structure, and a cost function. The plant (see Figure 1) is described in the time domain as

$$y(t) = P_d(q^{-1})u(t) + d(t) = \frac{B(q^{-1})}{A(q^{-1})}u(t) + \frac{1}{\nabla(q^{-1})A(q^{-1})}\psi_d(t), \tag{1}$$

where A, B, and ∇ are real polynomials, with A monic and $\nabla(q^{-1}) = 1 - q^{-1}$. The discrete-time transfer function $P_d = B/A$ is taken to be strictly causal, ie, the leading coefficient of B is zero. The signal y is the controlled variable (heart rate, HR), u is the plant control input (treadmill speed command, v), and d is an HR disturbance signal.

The term $d = (1/(\nabla A))\psi_d$ primarily represents physiological HR disturbances caused by broad-spectrum HRV.[10,14,15] Within the optimal control framework, the driving source ψ_d is considered to be a stochastic process, which enters the filter $1/(\nabla A)$ to generate d. Use of the integrating term $1/\nabla$ in the filter admits a range of disturbance types[13]: when the driver ψ_d is stationary white noise, d incorporates a random walk; when ψ_d is a nonstationary compound Poisson process,

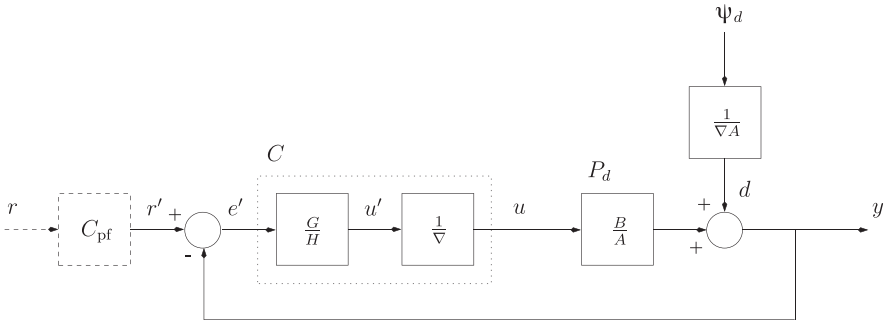

FIGURE 1 Plant model and control structure. The controlled variable y is the heart rate (HR); the control signal u is the treadmill speed command; and the reference signal r is the target heart rate (HR*). The term u' is the sample-to-sample change in the control signal: $u = (1/\nabla)u', \nabla = 1 - q^{-1} \Longleftrightarrow u'(t) = u(t) - u(t-1)$. The disturbance term d is modelled as a stochastic process ψ_d driving a shaping filter $1/(\nabla A)$. Transfer functions: P_d is the nominal plant, C is the feedback compensator, and C_{pf} is a deterministic reference prefilter

d includes a step-like sequence consisting of random steps at random times; and when ψ_d is a unit pulse, the output of the integrator is a deterministic step. By notionally combining such forms for ψ_d, practically relevant models for HRV arise.

In the sequel, the plant transfer function $P_d = B/A$ is taken to be a first-order LTI system; this assumption follows previous observations that such a model gives a good representation of HR dynamics during moderate-to-vigorous treadmill exercise,[11] and, further, that feedback control design based on this model structure can be highly accurate and robust.[10,12,16] Thus, with steady-state gain k and time constant τ, the transfer function for HR dynamics is represented in continuous and discrete forms as

$$u \to y : \; P_c(s) = \frac{k}{\tau s + 1} \overset{T_s}{\longleftrightarrow} P_d(z^{-1}) = \frac{B(z^{-1})}{A(z^{-1})} = \frac{b_0 z^{-1}}{1 + a_1 z^{-1}}, \tag{2}$$

where the double arrow denotes transformation between the continuous and discrete domains using sample period T_s. The discrete model parameters, expressed in k, τ, and T_s, are

$$a_1 = -e^{\frac{-T_s}{\tau}}, b_0 = k\left(1 - e^{\frac{-T_s}{\tau}}\right). \tag{3}$$

2.2 | Controller structure and cost function

The control signal u (here, the treadmill speed command signal) is generated by a causal linear feedback compensator transfer function C as $u(t) = C(q^{-1})e'(t)$, with $e'(t) = r'(t) - y(t)$ (Figure 1). The signal r' is the output of a deterministic reference prefilter C_{pf}, and r is the reference signal (target heart rate, HR*).

Integral action is specified in the compensator by constraining the denominator of C to include the factor $\nabla(q^{-1}) = 1 - q^{-1}$; this is in line with the internal model principle, which demands within the feedback path a model of the unstable dynamic structure of the disturbance d, viz, the term $1/\nabla$.[17] Thus, the compensator transfer function is described as

$$e' \to u \; : \; C(q^{-1}) = \frac{G(q^{-1})}{H(q^{-1})} \cdot \frac{1}{\nabla(q^{-1})}, \tag{4}$$

where G and H are real polynomials to be determined by the cost-function minimisation, with H monic.

The optimisation problem below is formulated by penalising sample-to-sample changes in the control signal, which are given by the intermediate signal u' (Figure 1) since

$$u(t) = \frac{1}{\nabla(q^{-1})}u'(t) \Longleftrightarrow u'(t) = \nabla(q^{-1})u(t) = u(t) - u(t-1). \tag{5}$$

The optimal feedback compensator C is obtained as the solution to a stochastic regulation problem, ie, under the assumption of zero reference signals $r = r' = 0$; reference tracking is introduced deterministically in the sequel via the reference prefilter C_{pf} (Section 2.5).

The optimal regulator polynomials G and H are those which minimise a quadratic cost function J, expressed in the time and frequency domains as

$$J = E\left\{y^2(t) + \rho u'^2(t)\right\} = \frac{1}{2\pi j}\oint_{|z|=1} (\phi_y + \rho\phi_{u'})\,\frac{dz}{z}, \tag{6}$$

where E denotes expectation, and ϕ_y and $\phi_{u'}$ are spectral densities. The real scalar ρ is the control weighting, which can be used as a single controller tuning parameter to establish a desired compromise between regulation accuracy and control signal activity: increasing ρ penalises control signal changes more heavily, resulting, nominally, in a less dynamic control signal and, correspondingly, less accurate output regulation, and vice versa. Equivalence of the time- and frequency-domain expressions in Equation 6 is established by application of Parseval's theorem.[18,19]

Equivalently, the cost function can be written in terms of $u = (1/\nabla)u'$ as

$$J = E\left\{y^2(t) + \rho(\nabla u)^2(t)\right\} = \frac{1}{2\pi j}\oint_{|z|=1}(\phi_y + \rho\nabla\nabla^*\phi_u)\,\frac{dz}{z}, \tag{7}$$

where ∇^* is the conjugate of ∇, ie, $\nabla^*(z^{-1}) = \nabla(z)$.

2.3 | Performance measures and relation to cost function

Recent studies on feedback control of HR have used quantitative measures of closed-loop control performance[10,12,16] and these measures are adopted in the present work. Tracking accuracy is assessed using the RMSE on an interval $[t_0, t_1]$

$$\text{RMSE} = \sqrt{\frac{1}{N}\sum_{t=t_0}^{t_1}(y_{\text{nom}}(t) - y(t))^2}, \tag{8}$$

where $N = t_1 - t_0 + 1$. The signal y_{nom} is the nominal simulated HR response from reference r to output y, $y_{\text{nom}} = C_{\text{pf}}T_o r$ (Figure 1, Equations 22 and 26).

The intensity of the control signal is quantified using the average power of changes in u, denoted $P_{\nabla u}$, where

$$P_{\nabla u} = \frac{1}{N-1}\sum_{t=t_0+1}^{t_1}(u(t) - u(t-1))^2. \tag{9}$$

For simplicity, this quantity is referred to henceforth as "average control signal power."

These expressions are closely related to the cost function $J = E\{y^2(t) + \rho u'^2(t)\}$ in Equation 6. In the case of pure regulation, ie, setting $y_{\text{nom}} = r = 0$, the term RMSE^2 from Equation 8 simplifies to RMSE$^2 = \frac{1}{N}\sum_{t=t_0}^{t_1} y^2(t)$, which is seen to be a sample estimate of the expectation $E\{y^2(t)\}$ in Equation 6. In a similar vein, $P_{\nabla u}$ provides a sample estimate of the second term $E\{u'^2(t)\}$ in the cost function (6). The control weighting ρ thus provides a natural means by which to adjust the relative importance of the 2 primary outcome measures, RMSE and $P_{\nabla u}$, in the manner outlined in Section 2.2 above.

2.4 | Optimal regulator solution

The optimal regulator polynomials G and H in Equation 4, which minimise the cost function J, Equations 6 and 7 satisfy the linear polynomial Diophantine equation

$$A\nabla H + BG = D_c, \tag{10}$$

where D_c, the characteristic polynomial of the feedback loop, is the strictly stable spectral factor obtained from

$$D_c D_c^* = BB^* + A\nabla\rho\nabla^* A^*. \tag{11}$$

For a proof of this result, see the works of Hunt[13] and Åström and Wittenmark[20] (ch. 12).

For a first-order plant $P_d(q^{-1}) = B(q^{-1})/A(q^{-1}) = b_0 q^{-1}/(1 + a_1 q^{-1})$, Equation 2 and with $\nabla = 1 - q^{-1}$, the degree of D_c in Equation 11 is $n_{dc} = 2$, ie,

$$D_c(q^{-1}) = 1 + d_{c1}q^{-1} + d_{c2}q^{-2}. \tag{12}$$

The unique minimal-degree solution of Equation 10 then has polynomial degrees $n_g = 1$ and $n_h = 0$, giving $G(q^{-1}) = g_0 + g_1 q^{-1}$ and $H(q^{-1}) = 1$.[13,20] The optimal regulator structure, for the first-order case, is therefore

$$C(q^{-1}) = \frac{G(q^{-1})}{H(q^{-1})}\cdot\frac{1}{\nabla(q^{-1})} = \frac{g_0 + g_1 q^{-1}}{1 - q^{-1}}. \tag{13}$$

An explicit solution for the feedback compensator parameters g_0 and g_1 can be readily obtained by writing out Equation 10 in full, viz,

$$(1 + a_1 q^{-1})(1 - q^{-1}) + b_0 q^{-1}(g_0 + g_1 q^{-1}) = 1 + d_{c1}q^{-1} + d_{c2}q^{-2}. \tag{14}$$

Equating coefficients of like powers and resolving for the unknowns gives

$$g_0 = (d_{c1} - a_1 + 1)/b_0, \tag{15}$$

$$g_1 = (d_{c2} + a_1)/b_0. \tag{16}$$

In summary, given the plant steady-state gain k and time constant τ, together with a sample period T_s, the optimal regulator is determined in the following steps:

1. Calculate $a_1 = -e^{(-T_s/\tau)}$ and $b_0 = k(1 - e^{(-T_s/\tau)})$, Equation 3.
2. Obtain d_{c1} and d_{c2} from spectral factorisation Equation 11, and using Equation 12.
3. Calculate $g_0 = (d_{c1} - a_1 + 1)/b_0$ and $g_1 = (d_{c2} + a_1)/b_0$, Equations 15 and 16.
4. Implement feedback compensator as $C(q^{-1}) = (g_0 + g_1 q^{-1})/(1 - q^{-1})$, Equation 13.

As an aside, it is noted that the optimal regulator structure for the first-order case, Equation 13, is equivalent to an ideal PI controller C_{PI} with proportional gain k_p and integrator gain k_i because, cf Equation 13,

$$e' \to u : \; C_{\mathrm{PI}}(q^{-1}) = k_p + \frac{k_i}{1 - q^{-1}} = \frac{(k_p + k_i) + (-k_p)q^{-1}}{1 - q^{-1}}. \tag{17}$$

Therefore,

$$C(q^{-1}) = C_{\mathrm{PI}}(q^{-1}) \Longleftrightarrow g_0 = k_p + k_i, \quad g_1 = -k_p \Longleftrightarrow k_p = -g_1, \quad k_i = g_0 + g_1. \tag{18}$$

2.5 | Reference prefilter

The strategy adopted here for the design of the deterministic reference prefilter C_{pf} was to retain in the overall closed-loop transfer function from reference r to plant output y the characteristic polynomial of the feedback loop, D_c, Equation 10, together with the plant zero polynomial B. Inclusion of B, which has the strictly causal term q^{-1}, ensures that C_{pf} will be causal (otherwise, a predictive factor would be required). Thus, it was required that

$$r \to y : \; \frac{D_c(1)}{B(1)} \cdot \frac{B(q^{-1})}{D_c(q^{-1})}, \tag{19}$$

where the scalar term $D_c(1)/B(1)$ enters to ensure an overall steady-state gain of unity.

The overall closed-loop transfer function from r to y is given by (see Figure 1)

$$r \to y \; : \; C_{\mathrm{pf}}(q^{-1}) \cdot \frac{B(q^{-1})G(q^{-1})}{D_c(q^{-1})}. \tag{20}$$

Equating expressions (19) and (20) and solving for C_{pf} gives, in general,

$$C_{\mathrm{pf}}(q^{-1}) = \frac{D_c(1)/B(1)}{G(q^{-1})}, \tag{21}$$

and for the first-order case

$$C_{\mathrm{pf}}(q^{-1}) = \frac{(1 + d_{c1} + d_{c2})/b_0}{g_0 + g_1 q^{-1}}. \tag{22}$$

2.6 | Pole-assignment design

For comparative purposes, a feedback compensator was also designed using a pole assignment (PA) method where the closed-loop poles were specified using the closed-loop rise time (this approach was also taken in previous works[12,16]). The feedback compensator transfer function was taken to be identical to that used in the optimal design, ie, $C(q^{-1}) = (g_0 + g_1 q^{-1})/(1 - q^{-1})$, Equation 13, but instead of using the optimal characteristic polynomial D_c obtained by spectral factorisation (11), D_c in Equation 12 was calculated using a desired 10%-90% closed-loop rise time t_r and critical relative damping $\zeta = 1$ to give (see the work of Hunt and Hunt[16])

$$d_{c1} = -2e^{-3.35T_s/t_r}, \quad d_{c2} = e^{-6.7T_s/t_r}. \tag{23}$$

All other details of the algebraic problem solution are then identical to the optimal case, ie, only step 2 of the 4-step algorithm summary in Section 2.4 differs for the PA design; the parameters d_{c1} and d_{c2} in Equation 12 are obtained from Equation 23 instead of from Equation 11. A reference prefilter was also used with the PA design; it was calculated according to Equation 22.

2.7 | Frequency-domain analysis

A key design issue for HR control is to ensure that broad-spectrum HRV, modelled here using the disturbance signal d, does not unduly excite the control signal u: physically, the control signal is the treadmill speed command, which is directly imposed upon and perceived by the runner.

The effect of the disturbance d on the control signal u can be analysed using the nominal input sensitivity function, denoted U_o, Equation 24 below, which is the transfer function linking these 2 signals (and between r' and u).

A further design goal is to achieve accurate HR regulation performance, ie, to keep the HR output y close to the reference $r(\mathrm{HR}^*)$. The degree to which the HRV disturbance d is suppressed by the feedback is determined by the sensitivity function S_o, Equation 25 below, which is the transfer function between d and y. Nominally, a greater degree of disturbance rejection corresponds to more accurate reference tracking but at the cost of higher control signal power. An appropriate compromise must therefore be reached between these 2 aspects; this trade-off can best be achieved by appropriate shaping of U_o and S_o.[10]

The complementary sensitivity function T_o, Equation 26, which governs the reference tracking response, is also defined below. In summary, the 3 key frequency response functions used in the sequel for controller design and performance interpretation are the following:

Input sensitivity function U_o

$$d \to u, r' \to u: \; U_o(z^{-1}) = \frac{C(z^{-1})}{1 + C(z^{-1})P_d(z^{-1})} = \frac{AG}{A\nabla H + BG} = \frac{AG}{D_c}; \tag{24}$$

Sensitivity function S_o

$$d \to y: \; S_o(z^{-1}) = \frac{1}{1 + C(z^{-1})P_d(z^{-1})} = \frac{A\nabla H}{A\nabla H + BG} = \frac{A\nabla H}{D_c}; \tag{25}$$

Complementary sensitivity function T_o

$$r' \to y: \; T_o(z^{-1}) = \frac{C(z^{-1})P_d(z^{-1})}{1 + C(z^{-1})P_d(z^{-1})} = \frac{BG}{A\nabla H + BG} = \frac{BG}{D_c}. \tag{26}$$

2.8 | Controller calculation

Three controllers were designed using an existing approximate plant model with $k = 24.2$ bpm/(m/s) and $\tau = 57.6$ seconds, and implemented using a sample period $T_s = 5$ seconds. This single model was obtained in a previous identification study as the average of 48 individual models estimated from 24 subjects, each running at moderate and vigorous intensity levels.[11] Thus, in the present study, no model identification was performed, and the nominal model was not specific to any of the subjects tested.

The nominal plant model, Equation 2, was

$$u \to y: \; P_c(s) = \frac{24.2}{57.6s + 1} \xleftrightarrow{T_s = 5s} P_d(z^{-1}) = \frac{b_0 z^{-1}}{1 + a_1 z^{-1}} = \frac{2.0121 z^{-1}}{1 - 0.9169 z^{-1}}. \tag{27}$$

Three different controllers, each comprising a feedback compensator of the form $C(q^{-1}) = (g_0 + g_1 q^{-1})/(1 - q^{-1})$, Equation 13, and a reference prefilter of the form Equation 22, were designed and tested with all subjects (controller summary in Table 1). Two optimal controllers were included to investigate the effect of the control weighting ρ on closed-loop performance. A standard PA design (Section 2.6) was included to facilitate direct comparison with one of the 2 optimal controllers; the second optimal controller, below, was parameterised to give similar loop characteristics to the PA controller.

The first controller used the PA design (Section 2.6) with closed-loop rise time $t_r = 150$ seconds, giving

$$C_1(q^{-1}) = \frac{0.06370 - 0.05815 q^{-1}}{1 - q^{-1}}. \tag{28}$$

TABLE 1 Controller parameterisation

Controller	Type	Setting
C_1	PA	$t_r = 150$ s
C_2	LQ	$\rho = 67\,000$
C_3	LQ	$\rho = 18\,100$

C_1, C_2, C_3: controllers 1, 2, and 3; Equations 28, 29, and 30; PA: pole assignment; t_r: closed-loop rise time, Section 2.6; LQ: linear quadratic (optimal); ρ: control weighting, Equations 6 and 7

The rationale for the choice $t_r = 150$ seconds was that the range 120 to 180 seconds was previously evaluated using the PA approach for HR control during outdoor running and found to give accurate and robust performance.[16]

The second controller used the optimal LQ design approach (Section 2.4). The control weighting was selected to give the same complementary sensitivity bandwidth as for the PA design, C_1 above, resulting in the same reference tracking response from r' to y (see T_o in Equation 26). By this method, the control weighting was found to be $\rho = 67\,000$, giving

$$C_2(q^{-1}) = \frac{0.03343 - 0.02970q^{-1}}{1 - q^{-1}}. \tag{29}$$

The third controller also used the optimal LQ design, but the control weighting was selected to give a loop gain $L_o = CP_d$ with the same 0 dB crossover frequency as for the PA design. This gave $\rho = 18\,100$, and

$$C_3(q^{-1}) = \frac{0.05457 - 0.04754q^{-1}}{1 - q^{-1}}. \tag{30}$$

The parameterisation of the 3 controllers is summarised in Table 1; their frequency responses U_o and S_o are displayed in Figure 2. The frequency response of a strictly proper (ie, low-pass) compensator, as used in the work of Hunt and Fankhauser,[10] is also shown for further consideration in the discussion.

It can be seen from the frequency responses (Figure 2) that PA controller C_1 and LQ optimal controller C_3, as intended, have very similar characteristics, albeit the LQ controller C_3 gives slightly more complex behaviour due to a complex-conjugate pair of poles resulting from the spectral factorisation (11) (the PA design gives 2 equal real poles). The optimal controller C_2, which has a much higher control weighting ρ than C_3, is clearly much less dynamic than C_1 and C_3 since the high-frequency gain of U_o and the bandwidth of S_o are both substantially lower than for the other 2 controllers.

3 | EXPERIMENTAL METHODS

3.1 | Subjects

Twelve healthy male subjects were recruited for comparative experimental evaluation of the 3 controllers (subject details in Table 2). Each subject was tested with all 3 controllers, C_1, C_2, and C_3, giving 36 tests in total, with each test taking place on a separate day. The study design was counterbalanced by computer randomisation of controller testing order for each subject. Because 6 unique sequences are possible for 3 test cases, viz, the set of test sequences TS = {123, 132, 213, 232, 312, 321}, the number of subjects $n = 12$ was purposely chosen to be a multiple of 6, and each individual test sequence in the set TS was repeated twice across the 12 subjects.

All procedures performed in this study in regard to the human participants were in accordance with the ethical standards of the local research committee: the study protocol was reviewed and approved by the Ethics Committee of the Swiss Canton of Bern. Informed consent was obtained from all individual participants.

3.2 | Equipment and test procedures

Experiments were performed using a computer-controlled treadmill (type Venus, h/p/cosmos Sports and Medical GmbH, Germany; Figure 3) and a chest belt for HR measurement (model T34, Polar Electro Oy, Finland).

All controller tests were performed in accordance with a formal protocol where each test lasted 35 minutes, and target HR was varied periodically by ± 10 beats per minute (bpm) around a mid-level (see Figures 5, 6, and 7). The mid-level HR was set individually for each subject to the value corresponding to the transition between moderate and vigorous

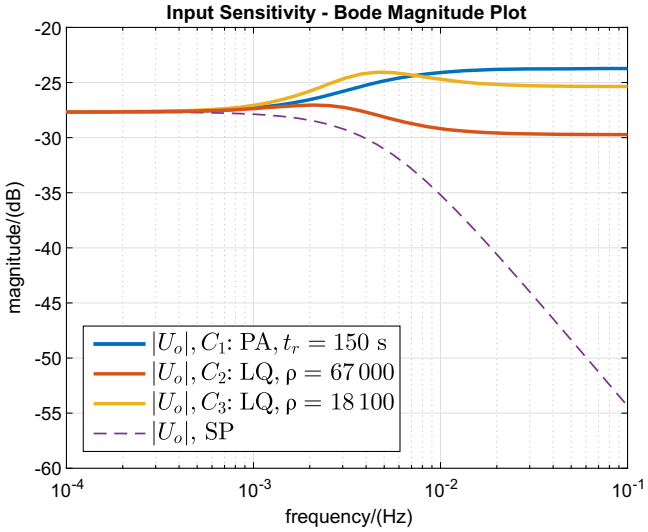

(A) Input sensitivity function magnitudes, $|U_o|$.

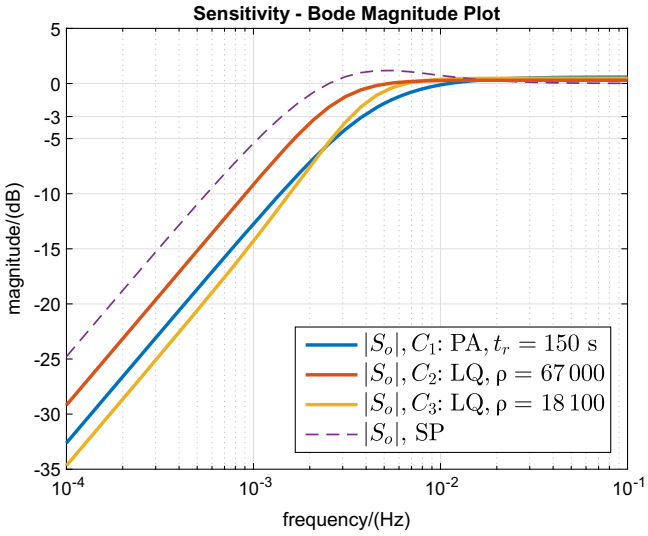

(B) Sensitivity function magnitudes, $|S_o|$.

FIGURE 2 Frequency responses for controllers C_1, C_2, and C_3 (solid lines). $|U_o|$, SP and $|S_o|$, SP (dashed lines) are for the strictly proper compensators used in the work of Hunt and Fankhauser.[10] LQ, linear quadratic; PA, pole assignment; ρ, control weighting; SP, strictly proper; t_r, rise time [Colour figure can be viewed at wileyonlinelibrary.com]

exercise intensity regimes, which is taken to be 76.5% of the age-predicted maximal HR, HR_{max}[2]; the latter was estimated as $HR_{max} = 220 - age$.[21] This experimental protocol is similar to that used in previous studies.[10,12]

3.3 | Primary outcome measures and statistical analysis

The primary outcome measures were RMSE, Equation 8 and average control signal power $P_{\nabla u}$, Equation 9. These outcomes were evaluated for all tests across the time interval $300 \leq t \leq 1800$ seconds (5 to 30 minutes; see Figures 5 to 7).

Both primary outcomes were statistically analysed to evaluate possible differences between the 3 controllers. One-way repeated-measures analysis of variance (ANOVA) was used, with controller number (1, 2, or 3) as the single factor. Whenever a significant overall difference was determined (overall p value), posthoc pairwise comparisons were performed for the pairs of controllers, with Bonferroni correction of significance levels. For paired comparisons, mean differences (MDs) and 95% confidence intervals were computed.

TABLE 2 Subject characteristics

	Age, y	Body Mass, kg	Height, m	BMI, kg/m^2
S01	52	75.4	1.85	22.0
S02	27	67.7	1.76	21.9
S03	24	75.2	1.81	23.0
S04	33	74.0	1.82	22.3
S05	22	73.5	1.78	23.2
S06	30	83.7	1.88	23.7
S07	22	59.0	1.71	20.2
S08	26	63.0	1.74	20.8
S09	32	75.0	1.78	23.7
S10	26	79.0	1.80	24.4
S11	23	68.0	1.83	20.3
S12	28	73.4	1.75	24.0
Mean ± SD	28.8 ± 8.2	72.2 ± 6.8	1.79 ± 0.05	22.5 ± 1.5
Range	22–52	59.0–83.7	1.71–1.88	20.2–24.4

BMI, body mass index (mass/height^2); $n = 12$, all male; SD, standard deviation

FIGURE 3 Computer-controlled treadmill. Controllers were implemented in real time in the PC on the left. The control signal (speed command) was sent via serial link to the treadmill control unit in the centre [Colour figure can be viewed at wileyonlinelibrary.com]

TABLE 3 Outcome measures for the 3 controllers and overall p values for comparison of means (see also Figure 4)

	Mean ± SD			p value
	C_1	C_2	C_3	
RMSE/(bpm)	2.12 ± 0.39	2.20 ± 0.38	2.22 ± 0.45	0.57
$P_{\nabla u}/(10^{-4}\ \mathrm{m}^2/\mathrm{s}^2)$	78.5 ± 21.4	22.6 ± 7.3	62.5 ± 14.0	5.1×10^{-9}

$n = 12$; SD: standard deviation; C_1, C_2, C_3: controllers 1 (PA), 2 (LQ, ρ = 67000), and 3 (LQ, ρ = 18100); p values: overall values, one-way repeated-measures ANOVAs; RMSE: root-mean-square tracking error; bpm: beats per minute; $P_{\nabla u}$: average power of changes in v

The null hypothesis was that no differences existed in the outcomes between the 3 controllers. The significance level for hypothesis testing was set to 5% ($\alpha = 0.05$). Statistical analysis was performed using the MATLAB Statistics and Machine Learning Toolbox (The Mathworks Inc, USA).

TABLE 4 Paired comparisons (differences) for root-mean-square tracking error (see also Table 3, first row of data, and Figures 4A-4B)

Comparison	MD (95% CI) /(bpm)	*p* value
$C_1 - C_2$	−0.09 (−0.34,0.16)	na
$C_1 - C_3$	−0.10 (−0.39,0.19)	na
$C_3 - C_2$	0.02 (−0.31,0.34)	na

$n = 12$; C_1, C_2, C_3: controllers 1 (PA), 2 (LQ, ρ = 67 000), and 3 (LQ, ρ = 18 100); MD: mean difference; 95% CI: 95% confidence interval for the mean difference, with Bonferroni correction; na: not applicable (overall p value > 0.05, Table 3, first row)

4 | RESULTS

Heart rate tracking accuracy did not differ significantly between the 3 controllers C_1, C_2, and C_3: mean RMSE/(bpm) was 2.12, 2.20, and 2.22, respectively (Table 3, first row, overall $p = 0.57$; Table 4, MDs and 95% confidence intervals; Figures 4A and 4B).

Average control signal power was significantly different between C_1, C_2, and C_3: mean $P_{\nabla u}/(10^{-4}\ \mathrm{m}^2/\mathrm{s}^2)$ was 78.5, 22.6, and 62.5, respectively (Table 3, second row, overall $p = 5.1 \times 10^{-9}$; Table 5; Figures 4C and 4D).

Paired comparisons for average control signal power (Table 5, Figure 4D) showed that mean $P_{\nabla u}$ was significantly lower for C_2 than for C_1 (MD/$(10^{-4}\ \mathrm{m}^2/\mathrm{s}^2) = 55.9$, $p = 4.1 \times 10^{-6}$), and for C_3 (MD/$(10^{-4}\ \mathrm{m}^2/\mathrm{s}^2) = 39.9$, $p = 2.3 \times 10^{-5}$). There was moderate evidence that mean $P_{\nabla u}$ was lower for C_3 than for C_1 (MD/$(10^{-4}\ \mathrm{m}^2/\mathrm{s}^2) = 16.0$, $p = 0.063$).

A selection of test results for controllers C_1, C_2, and C_3 are given in Figures 5, 6 , and 7, respectively. For each controller, the results which had the lowest, median, and highest values for RMSE across all subjects are shown.

5 | DISCUSSION

In this work, HR control was formulated within a stochastic optimal control framework, and, in an empirical investigation, 2 parameterisations of the optimal controller and a PA controller were compared using formal statistical analysis.

Heart rate tracking was very precise, with mean RMSE on the range 2.12 to 2.22 bpm. There was no significant difference in RMSE between the 3 controllers, despite the very substantial and significant differences in average control signal power, which lay in the range 22.6 to $78.5 \times 10^{-4}\ \mathrm{m}^2/\mathrm{s}^2$. Since, nominally, higher control signal activity would be expected to drive down RMSE, this result may indicate that, at this very high level of tracking precision, an empirical lower bound on the achievable RMSE is being approached. This observation is supported by a previous study where RMSE was similar to that reported here (mean RMSE of 2.29 bpm over 32 tests), and where even higher levels of average control signal power did not lead to any observable reduction in RMSE.[12]

Conversely, it was observed elsewhere that when average control signal power is lower than the levels seen in the present study, RMSE tends to increase[10] (mean $P_{\nabla u} = 16.0 \times 10^{-4}\ \mathrm{m}^2/\mathrm{s}^2$, mean RMSE = 2.96 bpm). The latter reference differed from the present work principally in that the compensator and input sensitivity transfer functions were purposely designed to be low-pass (see the dashed line in Figure 2A), thus explaining the lower value of $P_{\nabla u}$, and the sensitivity function bandwidth was relatively low (dashed line in Figure 2B), leading to higher RMSE.

The sensitivity function bandwidths for the 3 controllers tested here were substantially higher than for the low-pass compensator mentioned above (see the −3 dB cutoff in Figure 2B), thus giving lower RMSE values: since the sensitivity function S_o is the transfer function from disturbance d to controlled variable y, Equation 25, higher S_o bandwidths would be expected, nominally, to give progressively more suppression of disturbances and consequently lower RMSE. That this outcome was not observed here between the 3 controllers C_1, C_2, and C_3 lends further support to the concept of an empirical lower bound for RMSE, as put forth above.

On the other hand, the substantial and significant differences in observed average control signal power between the 3 controllers is consistent with the shapes of the input sensitivity function U_o (Figure 2A), which is the transfer function from disturbance d to control signal u, Equation 24. The high-frequency gain of U_o can be seen to increase on the order C_2, C_3, C_1, which is consistent with the increases in the respective average control signal power values of 22.6, 62.5, and $78.5 \times 10^{-4}\ \mathrm{m}^2/\mathrm{s}^2$ (Table 3).

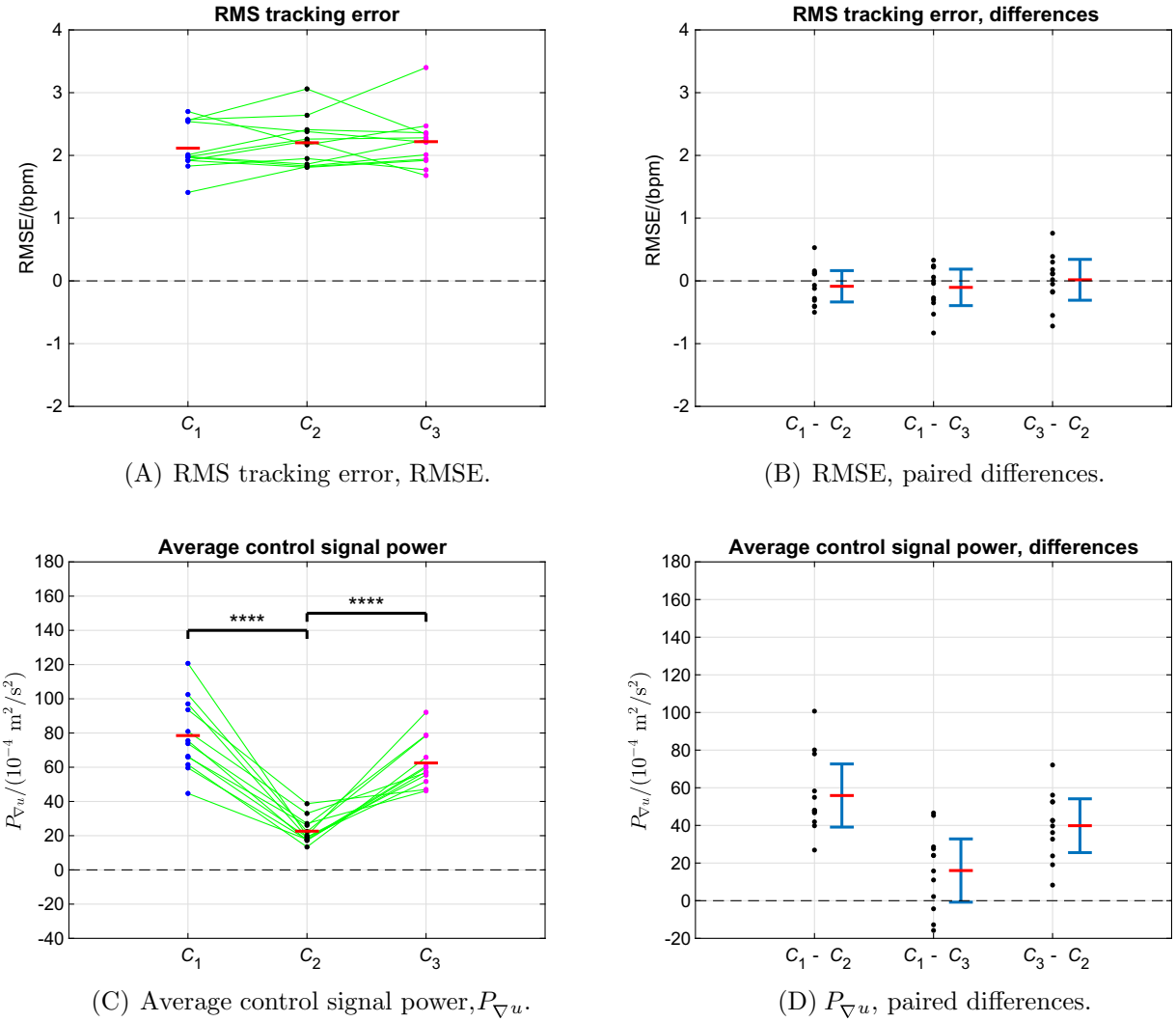

(A) RMS tracking error, RMSE.

(B) RMSE, paired differences.

(C) Average control signal power, $P_{\nabla u}$.

(D) $P_{\nabla u}$, paired differences.

FIGURE 4 Primary outcomes RMSE and $P_{\nabla u}$. Parts A and C: samples for all 12 subjects for the 3 controllers C_1, C_2, and C_3 (see also Table 3); the green lines link the sample pairs from each subject; the red horizontal bars depict mean values; **** $\iff p < 0.0001$ (paired comparisons, C_1 vs C_2 and C_2 vs C_3, in Tables 3 and 5). Parts B and D: sample differences for paired comparisons (see also Tables 4 and 5); the mean differences (MDs, red horizontal bars) and their 95% confidence intervals (CIs, blue) are shown beside the corresponding sample differences. Inclusion of value 0 within any 95% CI signifies a nonsignificant difference between the means, and vice versa (see also Tables 3 to 5) [Colour figure can be viewed at wileyonlinelibrary.com]

TABLE 5 Paired comparisons (differences) for average control signal power $P_{\nabla u}$(see also Table 3, second row of data, and Figures 4C-4D)

Comparison	MD (95% CI) /(10^{-4} m^2/s^2)	*p* value
$C_1 - C_2$	55.9 (39.1,72.6)	4.1×10^{-6}
$C_1 - C_3$	16.0 (−0.8,32.8)	0.063
$C_3 - C_2$	39.9 (25.6,54.1)	2.3×10^{-5}

$n = 12$; C_1, C_2, C_3: controllers 1 (PA), 2 (LQ, ρ = 67 000), and 3 (LQ, ρ = 18 100); MD: mean difference; 95% CI: 95% confidence interval for the mean difference, with Bonferroni correction; *p* value: paired comparison with Bonferroni correction

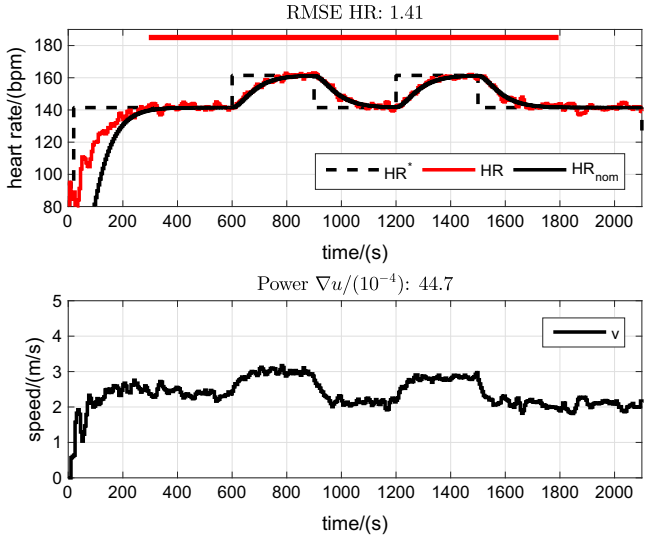

(A) Subject S05, lowest RMSE of 1.41 bpm, $P_{\nabla u} = 44.7 \times 10^{-4}$ m^2/s^2. HR$^* = 151.5 \pm 10$ bpm.

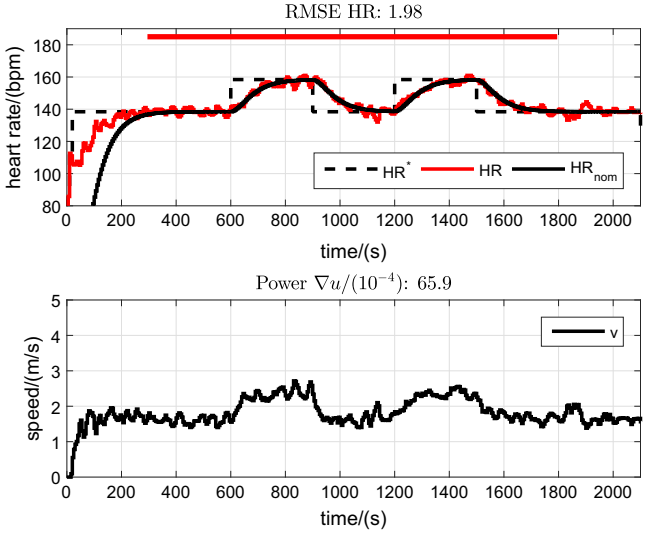

(B) Subject S08, median RMSE of 1.98 bpm, $P_{\nabla u} = 65.9 \times 10^{-4}$ m^2/s^2. HR$^* = 148.4 \pm 10$ bpm.

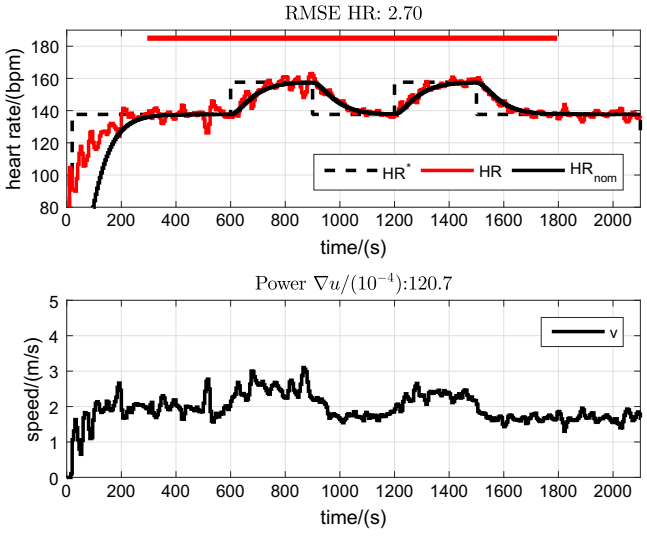

(C) Subject S02, highest RMSE of 2.70 bpm, $P_{\nabla u} = 120.7 \times 10^{-4}$ m^2/s^2. HR$^* = 147.6 \pm 10$ bpm.

FIGURE 5 Results with C_1 with the lowest (A), median (B), and highest (C) values for RMSE. In the upper part of each figure, HR* is the heart-rate reference, HR$_{\text{nom}}$ is the target nominal heart-rate response (simulated), and HR is the measured heart rate. In the lower graphs, v is the control signal, ie, the treadmill speed command. The thick red horizontal bars mark the outcome evaluation interval $300 \le t \le 1800$ seconds. RMSE, root-mean-square tracking error (Equation 8); $P_{\nabla u}$, average control signal power (Equation 9) [Colour figure can be viewed at wileyonlinelibrary.com]

The transfer functions of the 3 controllers C_1, C_2, and C_3 were purposely constrained here only to be causal and not strictly causal: see the structure of the general time-domain expression for $C(q^{-1})$ in Equation 13. This corresponds, in the frequency domain, to a transfer function $C(z^{-1})$ that is merely proper when expressed in z and not strictly proper. Consequently, the gain of C is not of low-pass character and does not roll-off to zero at high frequency. This non–low-pass frequency-domain behaviour of C carries over to the input sensitivity function U_o (see Equation 24), whence the observed non–low-pass shape of the 3 corresponding functions $|U_o|$ in Figure 2A.

This design choice, and the resultant frequency-domain characteristics of the key transfer functions, gives a relatively dynamic overall control system performance with a very low RMSE but relatively high average control signal power. This

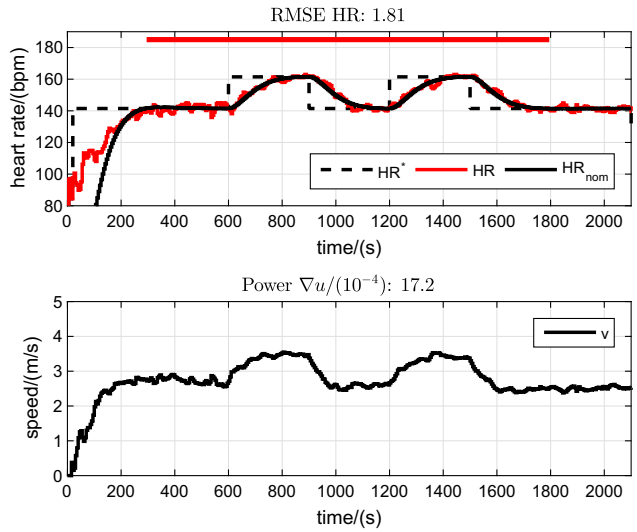

(A) Subject S07, lowest RMSE of 1.81 bpm, $P_{\nabla u} = 17.2\times 10^{-4}$ m^2/s^2. HR* = 151.5±10 bpm.

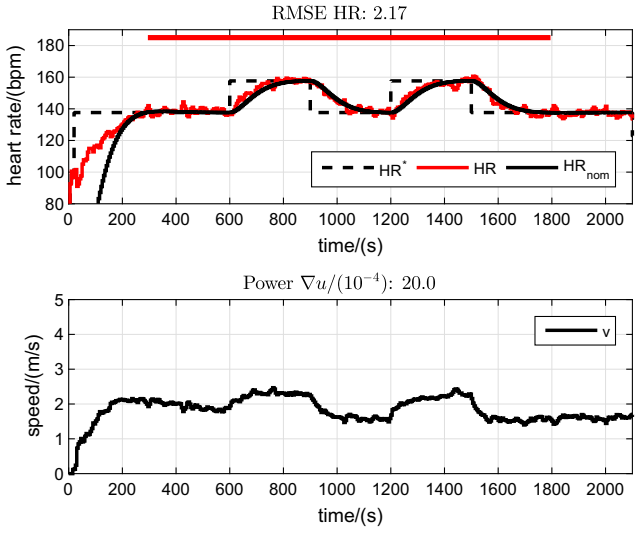

(B) Subject S02, median RMSE of 2.17 bpm, $P_{\nabla u} = 20.0\times 10^{-4}$ m^2/s^2. HR* = 147.6±10 bpm.

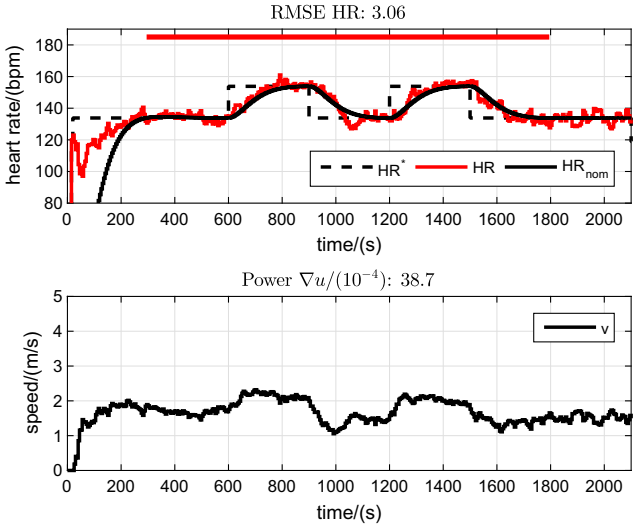

(C) Subject S09, highest RMSE of 3.06 bpm, $P_{\nabla u} = 38.7\times 10^{-4}$ m^2/s^2. HR* = 143.8±10 bpm.

FIGURE 6 Results with C_2 with the lowest (A), median (B), and highest (C) values for RMSE. In the upper part of each figure, HR* is the heart-rate reference, HR$_{\text{nom}}$ is the target nominal heart-rate response (simulated), and HR is the measured heart rate. In the lower graphs, v is the control signal, ie, the treadmill speed command. The thick red horizontal bars mark the outcome evaluation interval $300 \le t \le 1800$ seconds. RMSE, root-mean-square tracking error (Equation 8); $P_{\nabla u}$, average control signal power (Equation 9) [Colour figure can be viewed at wileyonlinelibrary.com]

is because the feedback loop retains the capability of generating corrective control signals across the whole range of the broad-spectrum HRV disturbance, by virtue of the absence of roll-off in $|U_o|$ (Figure 2A).

As noted above, constraining the controller and the input sensitivity function to be low-pass gives a much smoother control signal but higher RMSE.[10] The next logical step in the further development of the stochastic optimal control formulation of HR control would therefore be to extend the theory to achieve these characteristics, as they may be desirable in some application settings. Technically, this can be achieved by making the compensator transfer function (4) strictly causal, with the additional factor q^{-1} in the numerator along with the polynomial $G(q^{-1})$. Perusal of the characteristic Equation 10 reveals that at least 1 additional closed-loop pole, and at least 1 additional pole in C, would be required for a unique, optimal, and minimal-degree solution. This, in turn, can be obtained by modifying the nominal plant structure

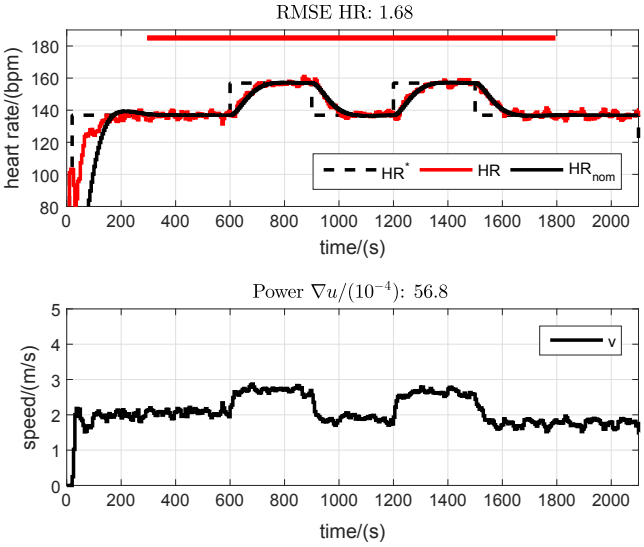

(A) Subject S12, lowest RMSE of 1.68 bpm, $P_{\nabla u} = 56.8 \times 10^{-4}$ m^2/s^2. HR*= 146.9±10 bpm.

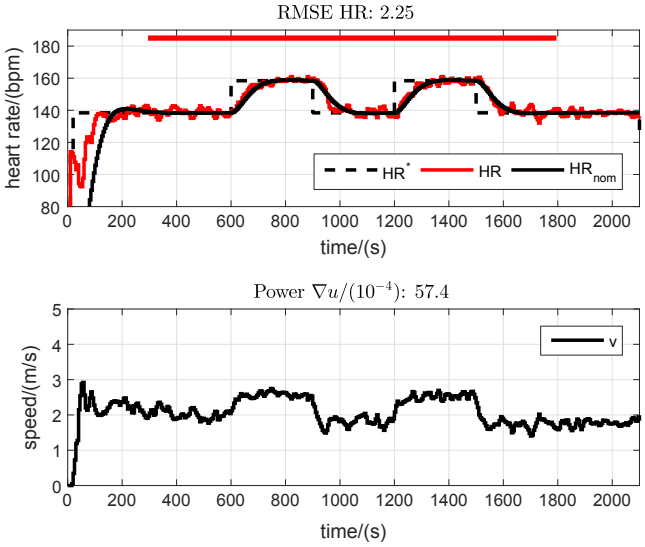

(B) Subject S10, median RMSE of 2.25 bpm, $P_{\nabla u} = 57.4 \times 10^{-4}$ m^2/s^2. HR* = 148.4±10 bpm.

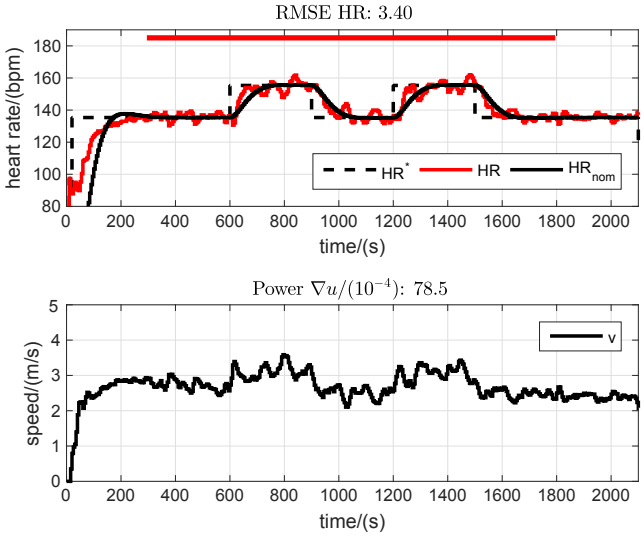

(C) Subject S06, highest RMSE of 3.40 bpm, $P_{\nabla u} = 78.5 \times 10^{-4}$ m^2/s^2. HR* = 145.4±10 bpm.

FIGURE 7 Results with C_3 with the lowest (A), median (B), and highest (C) values for RMSE. In the upper part of each figure, HR* is the heart-rate reference, HR$_{nom}$ is the target nominal heart-rate response (simulated), and HR is the measured heart rate. In the lower graphs, v is the control signal, ie, the treadmill speed command. The thick red horizontal bars mark the outcome evaluation interval $300 \le t \le 1800$ seconds. RMSE, root-mean-square tracking error (Equation 8); $P_{\nabla u}$, average control signal power (Equation 9) [Colour figure can be viewed at wileyonlinelibrary.com]

in Equation 1 to include a zero in the disturbance transfer function or by introducing a measurement noise term into the model[13]; the latter approach would lead to an additional spectral factorisation and to 2 additional closed-loop poles, thus giving faster high-frequency roll-off than would result from just 1 additional pole.

6 | CONCLUSIONS

The results of this study show that the stochastic optimal control framework provides a suitable method for attainment of highly accurate, stable, and robust control of HR during treadmill exercise. A single controller parameter, ie, the control

weighting factor ρ, can be used to set an appropriate balance between regulation accuracy and the intensity of the control signal. Moreover, the control weighting ρ has a clear and systematic influence on the shape of the input sensitivity function U_o. These features allow the physiological HRV disturbance to be dealt with appropriately and help ensure that changes in the control variable (treadmill speed) will be acceptable to the runner.

The results further demonstrate that a simple and approximate model of HR dynamics, used for the analytical design of an LTI controller of simple structure, can be sufficient for a high-quality HR control performance.

Future work should extend the stochastic optimal control problem formulation to encompass low-pass compensator and input sensitivity characteristics. It is also important to perform a sensitivity study to examine variations in the control weighting factor ρ and the corresponding trade-offs between performance and stability. The present study included a quite homogeneous group of male and predominantly young subjects. Further research is warranted to establish whether the control approach is robust in performance and stability when applied to other groups of subjects (eg, female subjects and other age groups).

DISCLOSURE STATEMENT

The authors declare that they have no conflict of interest.

AUTHORS' CONTRIBUTIONS

KJH designed the study. ML did the data acquisition. ML and KJH contributed to the analysis and interpretation of the data. KJH wrote the manuscript; ML revised it critically for important intellectual content. Both authors read and approved the final manuscript.

ORCID


Kenneth J. Hunt http://orcid.org/0000-0002-6521-9455

REFERENCES

1. Garber CE, Blissmer B, Deschenes MR, et al. American College of Sports Medicine position stand. Quantity and quality of exercise for developing and maintaining cardiorespiratory, musculoskeletal, and neuromotor fitness in apparently healthy adults: Guidance for prescribing exercise. *Med Sci Sports Exerc*. 2011;43(7):1334-1359.
2. Pescatello LS, Arena R, Riebe D, Thompson PD, eds. *ACSM's Guidelines for Exercise Testing and Prescription*. 9th ed. Philadelphia, USA: Lippincott, Williams and Wilkins; 2014.
3. Mezzani A, Hamm LF, Jones AM, et al. Aerobic exercise intensity assessment and prescription in cardiac rehabilitation. *Eur J Prev Cardiol*. 2013;20(3):442-467.
4. Weston M, Taylor KL, Batterham AM, Hopkins WG. Effects of low-volume high-intensity interval training (HIT) on fitness in adults: A meta-analysis of controlled and non-controlled trials. *Sports Med*. 2014;44(7):1005-1017.
5. Ramos JS, Dalleck LC, Tjonna AE, Beetham KS, Coombes JS. The impact of high-intensity interval training versus moderate-intensity continuous training on vascular function: A systematic review and meta-analysis. *Sports Med*. 2015;45(5):679-692.
6. Kawada T, Sunagawa G, Takaki H, et al. Development of a servo-controller of heart rate using a treadmill. *Jpn Circ J*. 1999;63(12):945-950.
7. Cheng TM, Savkin AV, Celler BG, Su SW, Wang L. Nonlinear modeling and control of human heart rate response during exercise with various work load intensities. *IEEE Trans Biomed Eng*. 2008;55(11):2499-2508.
8. Su SW, Huang S, Wang L, et al. Optimizing heart rate regulation for safe exercise. *Ann Biomed Eng*. 2010;38(3):758-768.
9. Scalzi S, Tomei P, Verrelli CM. Nonlinear control techniques for the heart rate regulation in treadmill exercises. *IEEE Trans Biomed Eng*. 2012;59(3):599-603.
10. Hunt KJ, Fankhauser SE. Heart rate control during treadmill exercise using input-sensitivity shaping for disturbance rejection of very-low-frequency heart rate variability. *Biomed Signal Process Control*. 2016;30(September):31-42. https://doi.org/10.1016/j.bspc.2016.06.005
11. Hunt KJ, Fankhauser SE, Saengsuwan J. Identification of heart rate dynamics during moderate-to-vigorous treadmill exercise. *BioMed Eng OnLine*. 2015;14:117. https://doi.org/10.1186/s12938-015-0112-7
12. Hunt KJ, Maurer RR. Comparison of linear and nonlinear feedback control of heart rate for treadmill running. *Syst Sci Control Eng*. 2016;4(1):87-98. https://doi.org/10.1080/21642583.2016.1179139
13. Hunt KJ. *Stochastic Optimal Control Theory with Application in Self-Tuning Control*. Lecture Notes in Control and Information Sciences, vol. 117. Berlin, Germany: Springer-Verlag; 1989.

14. Malik M, Bigger JT, Camm AJ, et al. Heart rate variability. Standards of measurement, physiological interpretation, and clinical use. *Eur Heart J*. 1996;17(3):354-381.
15. Sassi R, Cerutti S, Lombardi F, et al. Advances in heart rate variability signal analysis. *Europace*. 2015;17(9):1341-1353.
16. Hunt KJ, Hunt AJR. Feedback control of heart rate during outdoor running: A smartphone implementation. *Biomed Signal Process Control*. 2016;26(April):90-97. https://doi.org/10.1016/j.bspc.2016.01.001
17. Francis BA, Wonham WM. The internal model principle of control theory. *Automatica*. 1976;12(5):457-465.
18. Grimble MJ, Johnson MA. *Optimal Control and Stochastic Estimation: Theory and Applications*. New York, USA: Wiley; 1988.
19. Hunt KJ, ed. *Polynomial Methods in Optimal Control and Filtering*. IEE Control Engineering Series, vol. 49. Stevenage, UK: Peter Peregrinus; 1993.
20. Åström KJ, Wittenmark B. *Computer Controlled Systems: Theory and Design*. 3rd ed. Mineola, New York, USA: Dover Publications; 2011.
21. Shargal E, Kislev-Cohen R, Zigel L, Epstein S, Pilz-Burstein R, Tenenbaum G. Age-related maximal heart rate: Examination and refinement of prediction equations. *J Sports Med Phys Fitness*. 2015;55(10):1207-1218.

How to cite this article: Hunt KJ, Liu M. Optimal control of heart rate during treadmill exercise. *Optim Control Appl Meth*. 2018;39:503–518. https://doi.org/10.1002/oca.2355